Modulation of the Tibetan Plateau Snow Cover on the ENSO Teleconnections: From the East Asian Summer Monsoon Perspective

ZHIWEI WU

Key Laboratory of Meteorological Disaster, Ministry of Education, Nanjing University of Information Science and Technology, Nanjing, and State Key Laboratory of Numerical Modeling for Atmospheric Sciences and Geophysical Fluid Dynamics, Institute of Atmospheric Physics, Chinese Academy of Sciences, Beijing, China

JIANPING LI

State Key Laboratory of Numerical Modeling for Atmospheric Sciences and Geophysical Fluid Dynamics, Institute of Atmospheric Physics, Chinese Academy of Sciences, Beijing, China

ZHIHONG JIANG AND TINGTING MA

Key Laboratory of Meteorological Disaster, Ministry of Education, Nanjing University of Information Science and Technology, Nanjing, China

(Manuscript received 4 March 2011, in final form 9 August 2011)

ABSTRACT

The East Asian summer monsoon (EASM) may exhibit rather large variability between years characterized by the same ENSO phase. Such inconsistency reduces the EASM predictability based on ENSO. Results in this study show that the Tibetan Plateau snow cover (TPSC) exerts a modulating effect on ENSO teleconnections and ENSO significantly correlates with the EASM only during the reduced TPSC summers. Three-dimensional circulation structures are examined to manifest that the typical ENSO signals in reduced TPSC summers tend to be stronger than in excessive TPSC summers. Numerical and theoretical evidences indicate that the anomalously reduced TPSC can force positive geopotential height anomalies at the upper troposphere and weaken the jet streams across eastern Asia and northwestern Pacific. Governed by such basic state zonal flows, the extratropical Rossby wave response to the ENSO forcing usually has a larger amplitude and pronounced westward development. In such case, ENSO extends its influences to eastern Asia and enhances its connection with the EASM.

1. Introduction

It has been generally recognized that the East Asian summer monsoon (EASM) experiences strong interannual variations associated with the El Niño–Southern Oscillation (ENSO) (e.g., Fu and Teng 1988; Weng et al. 1999; Wang et al. 2000, 2008c; Chang et al. 2000a,b; Yang and Lau 2006). In light of this, ENSO is regarded as one principal predictability source for the EASM (e.g., Wang et al. 2008b; Wu and Li 2008; Wu et al. 2009). Nevertheless, the relationship between the EASM and ENSO is not stable and exhibits considerable interdecadal differences (e.g., Wang et al. 2008d, 2009; Li et al. 2010; Wu et al. 2012). Such inconsistency necessarily undermines ENSO-related long-range EASM predictability. Therefore, understanding the interdecadal modulation of ENSO teleconnections may facilitate the practical seasonal to decadal prediction of the EASM.

Many factors can modulate ENSO behavior on the decadal to interdecadal time scales. For instance, Gershunov and Barnett (1998) found that the North Pacific Oscillation (NPO) exerts a modulating effect not only on North American climate anomalies but also ENSO teleconnections. Yeh et al. (2009) proposed that a flattening of the thermocline in the equatorial Pacific can increase the occurrences of the central Pacific El Niño and, in turn, lead to the decadal changes in the associated atmospheric teleconnection patterns. Wu et al. (2012) suggested that

Corresponding author address: Dr. Zhiwei Wu, Key Laboratory of Meteorological Disaster, Ministry of Education, Nanjing University of Information Science and Technology, 219 Ningliu Rd., Nanjing 210044, China.
E-mail: zhiweiwu@hawaii.edu

DOI: 10.1175/JCLI-D-11-00135.1

the North Atlantic Oscillation (NAO) may also modify ENSO influence as well as its linkage with the EASM through exciting a distinct Rossby wave train prevailing over northern Eurasia and a simple Gill–Matsuno-type quadrupole response over the western Pacific. In addition, interdecadal changes in the magnitude and periodicity of ENSO, itself, may alter the local monsoon–ocean interactions in low latitudes and the impact on its linkage with the EASM (Wang et al. 2008d).

The impacts of Tibetan Plateau snow cover (TPSC) on regional climate (eastern Asia in particular) have been investigated by some studies (e.g., Ye 1981; Tao and Ding 1981; Zhang et al. 2004; Wu and Kirtman 2007; Wang et al. 2008a; Lin and Wu 2011). The Tibetan Plateau represents the highest elevated land on earth with an averaged elevation of more than 4000 m above sea level. With the highest mountains in the world, the TPSC can persist through the warm seasons over the high altitudes (Pu et al. 2007), making it a potential predictability source for summer climate in many places (Lin and Wu 2011), especially eastern Asia.

The influence of the Tibetan Plateau diabatic heating to EASM variability can be reflected by modifying the western Pacific subtropical high (WPSH), a principal component of the EASM system (e.g., Zhang et al. 2004; Wang et al. 2008a). Tao and Ding (1981) suggested that the diabatic heating over the western Tibetan Plateau may play a different role from that over the eastern Tibetan Plateau in affecting the WPSH. The response of the EASM to ENSO is qualitatively similar, namely, also through deforming the WPSH (Wang et al. 2000). This similarity of the EASM responses to Tibetan Plateau diabatic forcing and ENSO suggests that the more slowly involving TPSC interdecadal changes may modulate the ENSO-related EASM variability.

In this study, we attempt to answer the following questions. To what extent can the TPSC modulate ENSO teleconnections and in turn modify the ENSO–EASM relationship? What kind of physical mechanism is responsible for such modulation? This paper is structured as follows. Section 2 describes the datasets and model used in this study. The observed TPSC evolution for the 1968–2009 period is introduced in section 3, as well as the observed changes in the EASM and its linkage with simultaneous ENSO. Section 4 investigates the modulation effects of the TPSC on the relationship between ENSO and the EASM. A global primitive equation mode is utilized to assess the mechanisms in section 5. The last section summarizes major findings.

2. Data and model

In this study, we used monthly snow cover area extent data for 1968–2009 obtained from the Global Snow Laboratory (Rutgers University) and the National Centers for Environmental Prediction reanalysis version 1 (NCEP-1) (Kalnay et al. 1996) data for the 1968–2009 period. The sea surface temperature (SST) data were derived from the Extended Reconstructed SST Version 2 (ERSST V2) data (Smith and Reynolds 2004). The precipitation data were taken from the monthly global land precipitation (PREC/L) data gridded at $1.0° \times 1.0°$ resolution (Chen et al. 2002).

The Niño-3.4 index, defined as the SST anomaly (SSTA) averaged within the region (5°S–5°N, 170°–120°W), is used to quantify ENSO. The EASM index is calculated based on the definition by Wang et al. (2008c), which is the U_{850} in (22.5°–32.5°N, 110°–140°E) minus U_{850} in (5°–15°N, 90°–130°E) (where U_{850} denotes the zonal wind at 850 hPa). In this study, summer refers to June–August (JJA).

All numerical experiments are performed with a simplified general circulation model (SGCM) first developed by Hoskins and Simmons (1975). The resolution used here is triangular 31 with 10 equally spaced sigma levels (Lin and Derome 1996). An important feature of this model is that it uses a time-averaged forcing calculated empirically from observed daily data. The advantage of this SGCM model is that dynamical mechanisms are more easily isolated. As shown in Hall (2000), this model is able to reproduce remarkably realistic stationary planetary waves and the broad climatological characteristics of the transients are in general agreement with observations. The limitation of this approach is that the physical parameterizations present in GCMs are replaced by empirically derived terms, so some potentially important physical feedback mechanisms may be absent from our analysis.

3. Interdecadal changes in the TPSC and ENSO–EASM relationship

Shown in Fig. 1a is the summer climatology and standard deviation (STD) of the year-to-year variability of the TPSC. The major snow cover areas in summer are basically located in the western and southern Tibetan Plateau regions, which have higher altitudes and therefore, are favorable for the snow cover to persist through summer. Most of the interior of the plateau with lower altitudes has relatively less snow cover persistence. A strong STD center occupies the western plateau. Strong variability also exists in the southern flank of the plateau. Such notable year-to-year snow cover changes yield significant low boundary forcing signals for the atmosphere. In light of this, to quantitatively measure the strength of the TPSC forcing, a TPSC index (TPSI) is defined as the snow cover averaged within the domain (31°–41°N,

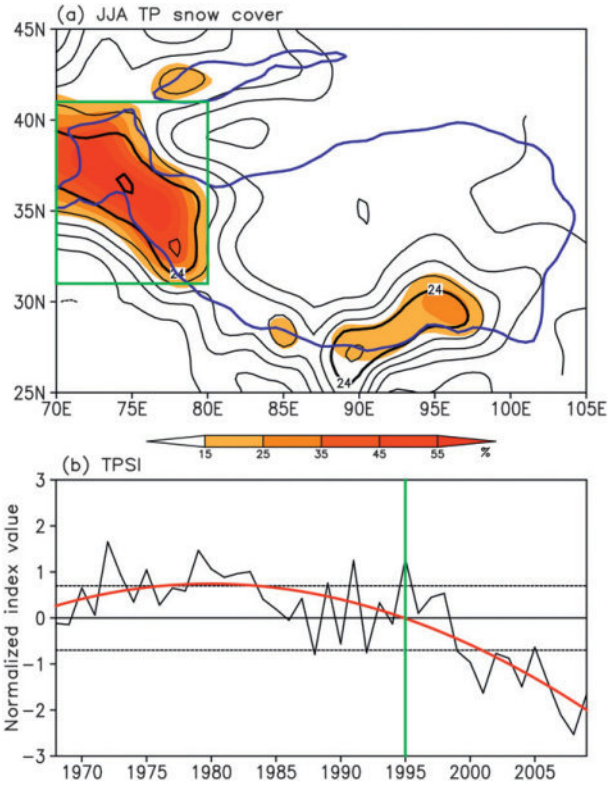

FIG. 1. (a) Long-term average (contours) and standard deviations (%) (color shading) of the Tibetan Plateau snow cover during summer [Jun–Aug (JJA)] for the period 1968–2009. The areas included by the blue curves are 3000 m MSL. (b) The normalized TPSC index (TPSI) time series (black curve) defined by the TPSC averaged in the green-boxed area in (a). The red curve indicates a third-order polynomial fit.

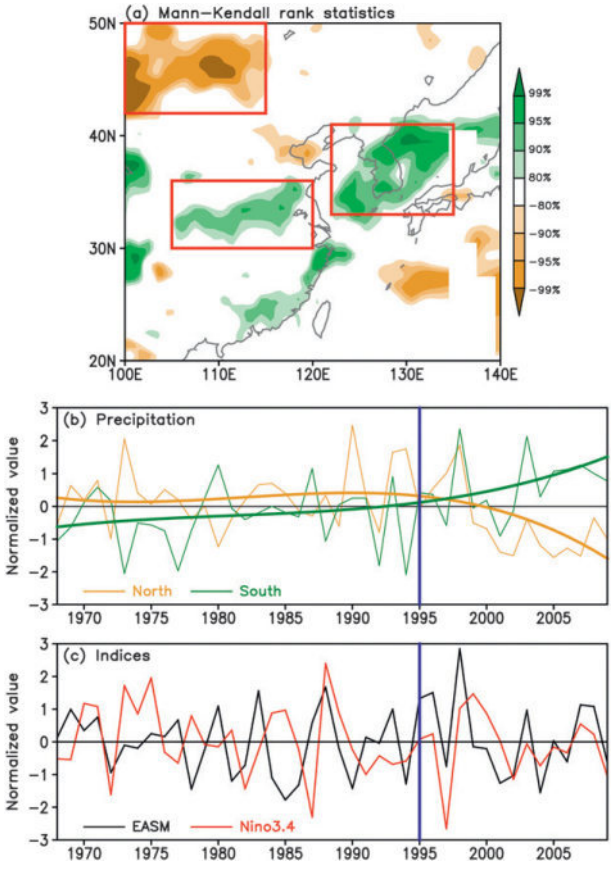

FIG. 2. (a) Mann–Kendall statistical significance of the linear trends in JJA precipitation over East Asia. (b) Time series of the normalized precipitation anomalies averaged over the northern [represented by the upper red box in (a), thin brown curve] and the southern [represented by the two lower red boxes in (a), thin green curve] East Asia. The thick curves indicate a third-order polynomial fits. (c) Time series of the normalized East Asian summer monsoon and JJA Niño-3.4 indices for the 1968–2009 period.

70°–80°E) where the summer climatology center and the year-to-year variability maximum are located (green box in Fig. 1a).

Figure 1b presents the time series of the normalized TPSI for the past 42 summers (1968–2009). A prominent feature is that the TPSC exhibits a pronounced interdecadal change; namely, the snow cover is significantly reduced after 1995. This point is further tested by the Lepage test (Yonetani 1992), which passes the 99% confidence level. Therefore, the earlier epoch (1968–95) is regarded as the excessive TPSC epoch, whereas the latter epoch (1996–2009) as the reduced TPSC epoch. If summers with a normalized TPSI > 0.7 (< -0.7) are considered to be anomalous, there are 11 excessive snow cover summers (1972, 1973, 1975, 1979, 1980, 1981, 1982, 1983, 1989, 1991, and 1995) and 12 reduced snow cover summers (1988, 1992, 1999, 2000, 2001, 2002, 2003, 2004, 2006, 2007, 2008, and 2009) for the 1969–2009 period. Note that our choice of 0.7 standard deviation as a threshold is just to obtain enough statistical samples for the following composite analysis.

Similar to the TPSC, Fig. 2a indicates that the EASM rainfall also experiences an interdecadal change over the northern and southern domain, respectively. The northern region shows a significant drought tendency, while the mei-yu–baiu–changma region displays an anomalous flooding trend. Such a drought–flood shift occurs around 1995, which exceeds the 99% confidence level based on the Lepage test. This precipitation pattern is somewhat similar to the meridional seesaw mode revealed by Zhu et al. (2007). The interdecadal alternation in both northern droughts and southern floods occurs after 1995 (Fig. 2b). As a matter of fact, Kwon et al. (2007) found that there is an interdecadal shift in the EASM around the mid-1990s. Wang et al. (2008a) attributed such a shift to the Tibetan Plateau warming. This study will not focus on how the TPSC affects the EASM rainfall.

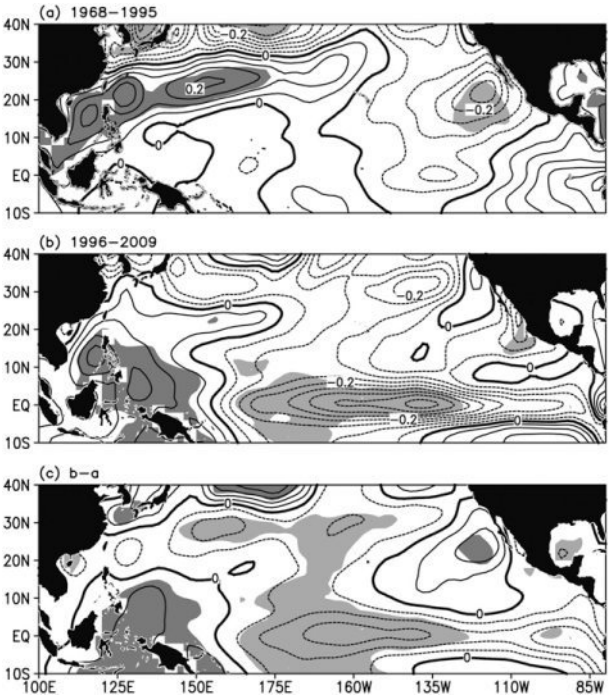

FIG. 3. The JJA sst anomaly (SSTA) (contours: °C) pattern regressed to the EASM index for the (a) 1968–95 and (b) 1996–2009 period and (c) the difference (b) minus (a). The dark (light) areas exceed the 95% confidence level.

Besides the EASM rainfall change, it is interesting to notice that the relationship between ENSO and the EASM also changes around 1995 (Fig. 2c). Before 1995, there is almost no linkage between the EASM and simultaneous ENSO, with the correlation coefficient between the JJA Niño-3.4 index and EASM index being −0.04. After 1995, the ENSO–EASM connection becomes rather intimate, with their correlation coefficient being −0.53 and exceeding 95% confidence level. The interdecadal change in the ENSO–EASM relationship around 1995 can also be supported by Fig. 3. During the earlier epoch (excessive TPSC), the simultaneous SSTA related to the EASM is basically in the northwestern Pacific, and no significant SSTA can be discerned in the equatorial Pacific (Fig. 3a). During the latter epoch (reduced TPSC), large areas of SSTAs emerge in the equatorial central-eastern Pacific (Fig. 3b). The SSTA difference between the two epochs displays a typical developing phase of La Niña (Fig. 3c). All of these indicate an enhanced linkage between the EASM and ENSO since 1995.

4. The TPSC modulation

Table 1 presents how the TPSC modulates the ENSO–EASM relationship. During the high TPSI (or excessive TPSC) summers, the EASM can be stronger or weaker than normal regardless of the ENSO phase ENSO. By contrast, during the low TPSI (or reduced TPSC) summers, a strong (weak) EASM prefers a La Niña (El Niño) phase. Among four low TPSI–El Niño summers, three summers have weaker than normal EASM (less than −0.5 STD), with two of them less than −1 STD, whereas among four high TPSI–La Niña summers, two of them have near normal EASM and two much stronger EASM (greater than 1 STD).

TABLE 1. Classification of summers based on phases of ENSO and the TPSI. Numbers within parentheses are the normalized EASM index values of the corresponding JJA.

Phase	High TPSI	Low TPSI
El Niño	1972 (−0.94), 1977 (0.67), 1982 (−0.71), 1991 (0.14)	2002 (−1.03), 2004 (−1.55), 2009 (−0.63)
La Niña	1970 (0.35), 1973 (−0.1), 1975 (0.25), 1978 (−1.45), 1989 (−0.2), 1.98 (2.85)	1988 (1.68), 1999 (−0.15), 2000 (−0.21), 2007 (1.13)

To further reveal the modulating effects of the TPSC on the ENSO teleconnections, first we investigate interdecadal changes in the three-dimensional circulation structures associated with the EASM. The extratropical 200-hPa geopotential height (H_{200}) anomalies are primarily confined over the oceanic areas during the earlier epoch (Fig. 4a). For example, an anomalously negative H_{200} anomaly belt is centered near the Japanese islands and extends eastward. At its equatorward side, there is an anomalously positive H_{200} anomaly belt. Over the eastern Eurasian continent, the H_{200} anomalies are rather weak in the extratropics (north of 30°N). For the latter epoch, significant H_{200} anomalies expand from the North Pacific into the extratropical eastern Eurasian continental areas, with two positive centers 1) located across the Sea of Okhotsk and 2) the region northwest of the Tibetan Plateau. These features are particularly clear in the difference map between the two epochs (Fig. 4c).

Figure 5 shows the large-scale sea level pressure (SLP) anomalies associated with the EASM. For the earlier epoch (Fig. 5a), the SLP anomalies over the North Pacific have the same sign with the H_{200} anomalies, which indicates a barotropic structure over the oceanic areas. This barotropic structure reflects that the anomaly is an extratropical response to a remote forcing. By contrast, the SLP anomalies during the latter epoch (Fig. 5b) have opposite sign with the H_{200} anomalies over the tropical central-eastern Pacific (Fig. 4b), so does the SLP and H_{200} differences between the two epochs (Figs. 5c and 4c). Such a baroclinic structure can be interpreted as atmospheric responses to the ENSO-related diabatic

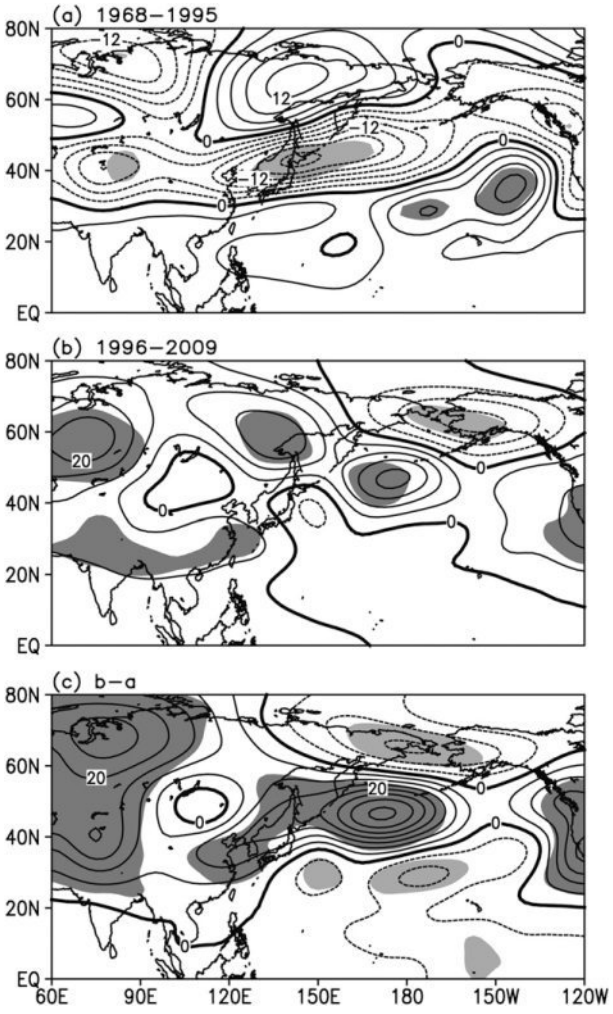

FIG. 4. As in Fig. 3, but for the JJA 200-hPa geopotential height (H_{200}) anomalies regressed to the EASM index.

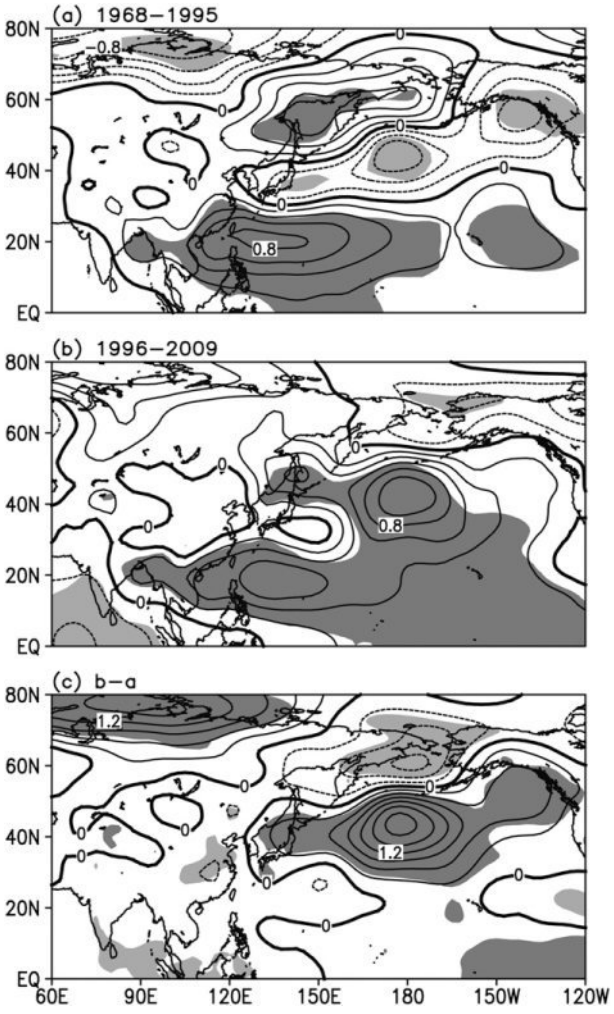

FIG. 5. As in Fig. 3, but for the JJA sea level pressure (SLP) anomalies anomalies regressed to the EASM index.

forcing of which the maximum heating area is located near the 300-hPa level (Lin 2009; Wu et al. 2012).

Based on the above analysis, we may infer that much stronger ENSO-related signals can be detected in the large-scale three-dimensional circulation structure associated with the EASM during the latter epoch. To understand the cause of such change, we examined the ENSO-related teleconnection patterns during the two epochs (Fig. 6). In general, the atmosphere in both epochs resembles a Gill-type response to the ENSO-related diabatic forcing located near equatorial central-eastern Pacific (Gill 1980). The circulation is quite symmetric about the equator. The notable difference is that the extratropical Rossby wave response during the latter epoch is stronger and more obvious over East Asia (Figs. 6b and 6c) than that during the earlier epoch (Fig. 6a). Lin (2009) suggested that the extratropical Rossby wave response of the atmosphere to the tropical diabatic forcing (i.e., ENSO) is largely determined by the summertime large-scale background mean flows. Therefore, whether the TPSC can modulate ENSO teleconnections largely depends on whether the TPSC is able to modify the summertime large-scale background mean flows.

Figure 7 shows the composite differences of H_{200} between the low and high TPSI summers defined in section 3 (low minus high). A salient positive difference center occupies the region north of the Tibetan Plateau and expands eastward toward the North Pacific. This may be interpreted as follows. A reduced (excessive) snow cover usually would favor high (low) H_{200} anomalies due to increased (reduced) solar radiation absorption at the surface and enhanced (suppressed) sensible heat and radiative fluxes from the ground. On the other hand, the high (low) H_{200} anomalies and warm (cold) upper-tropospheric

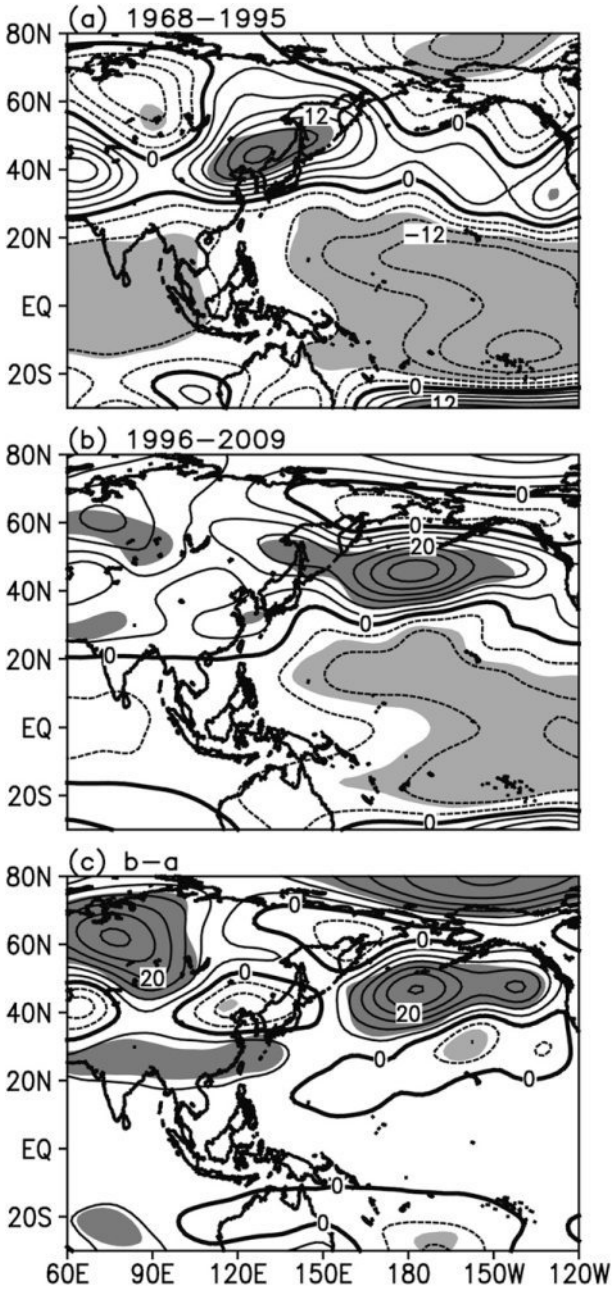

FIG. 6. As in Figs. 4a,b, but for the Niño-3.4 index. For comparison, the sign of the Niño-3.4 index is reversed.

temperature anomalies induced by the snow cover anomaly would produce decreased (increased) upper-tropospheric potential vorticity (Hoskins et al. 1985; Shaman and Tziperman 2005). Anomalous surface divergence (convergence) as well as anomalous vertical motions would follow, which would lead to decreased (increased) cloudiness and decreased (increased) precipitation in the region. This maintains the reduced (excessive) snow cover

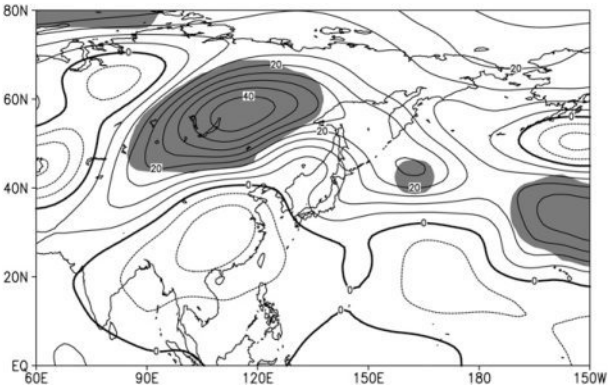

FIG. 7. Composite differences of H_{200} between the reduced and excessive TPSC JJA (reduced minus excessive). A reduced (excessive) TPSC JJA refers to that of a TSCI value greater (less) than 0.7 (−0.7) times the standard deviation.

anomalies. Such positive feedback may sustain such an atmosphere–snow cover anomaly pattern.

Coupled with the above positive H_{200} difference center, the 200-hPa zonal winds exhibit a dipole pattern that exactly corresponds to an anticyclonic wind anomaly (Fig. 8). The easterly wind differences prevail over the northern flank of the Tibetan Plateau and northeastern Asia and tilt southeastward toward the central North Pacific. Such a zonal wind distribution tends to decelerate (accelerate) the background mean westerly winds during the reduced (excessive) TPSC summers. This can be further confirmed by Fig. 9. The zonal wind speed averaged in (30°–55°N, 100°E–160°W) is ~16 m s^{-1} for the reduced TPSC summers and 17 m s^{-1} for the excessive TPSC summers.

Based on the above statistical analysis, we may speculate that the TPSC may modulate ENSO teleconnections and their linkage with the EASM through changing the background mean westerly winds over eastern Asia and the North Pacific.

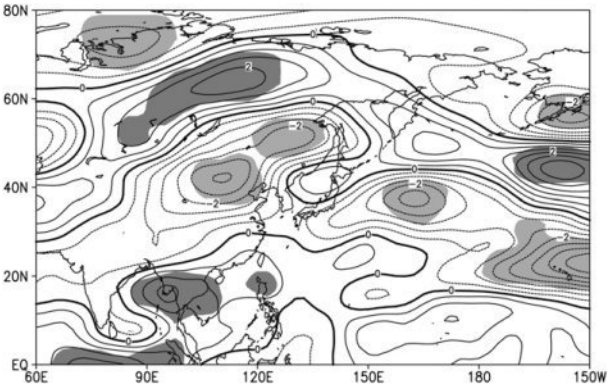

FIG. 8. As in Fig. 7, but for the 200-hPa zonal wind anomalies.

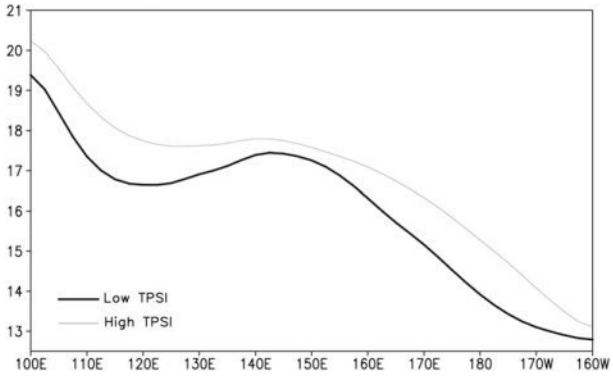

FIG. 9. JJA composite 200-hPa zonal winds averaged between 30° and 55°N. The thin (thick) curves indicate the high (low) TPSI JJA.

5. Numerical experiments and theoretical analysis

To further verify the above speculation, we conducted numerical experiments with the SGCM. Under the same ENSO forcing (a La Niña–related forcing here) we performed the experiments with a reduced TPSC anomaly, and excessive TPSC anomaly, and no TPSC anomaly, respectively. To mimic the diabatic heating effects of a reduced (excessive) TPSC anomaly we imposed one heating (cooling) anomaly source that has an elliptical squared cosine distribution in latitude and longitude. Based on the previous work by Hoskins and Karoly (1981), the vertically integrated heating (cooling) rate of the TPSC imposed here is 1.25 K day^{-1} (approximately the latent heating rate released by an extra 5-mm precipitation per day), and that of La Niña 2.5 K day^{-1} (approximately the latent heating rate released by an extra 10-mm precipitation per day). The vertical heating profile of the TPSC is $\sigma^4 \sin(\pi\sigma)$, peaking at around 400 hPa, while that of the ENSO is $(1 - \sigma) \sin[\pi(1 - \sigma)]$ and peaks around 300 hPa (Wu et al. 2009, 2012). Three perturbed experiments were integrated for 3700 days. The last 3600-day integrations were used to construct an ensemble (arithmetic) mean. Note that the result is not sensitive to the selection of initial condition since the analysis is conducted for the period after the climate equilibrium is reached.

It can be clearly seen from Fig. 10a that, under an excessive TPSC forcing, the 150-hPa geopotential height (H_{150}) basically exhibits a weakened extratropical Rossby wave response to the ENSO forcing over the region north of the Tibetan Plateau and the North Pacific, compared to the no-TPSC-anomaly experiment (Fig. 10c). In contrast, under a reduced TPSC forcing the extratropical Rossby wave response is stronger and more obvious over East Asia (Fig. 10b). Meanwhile, the 150-hPa zonal winds over these areas respond to easterly wind anomalies (Fig. 11). The consistency between the results from the numerical experiments and from the observations

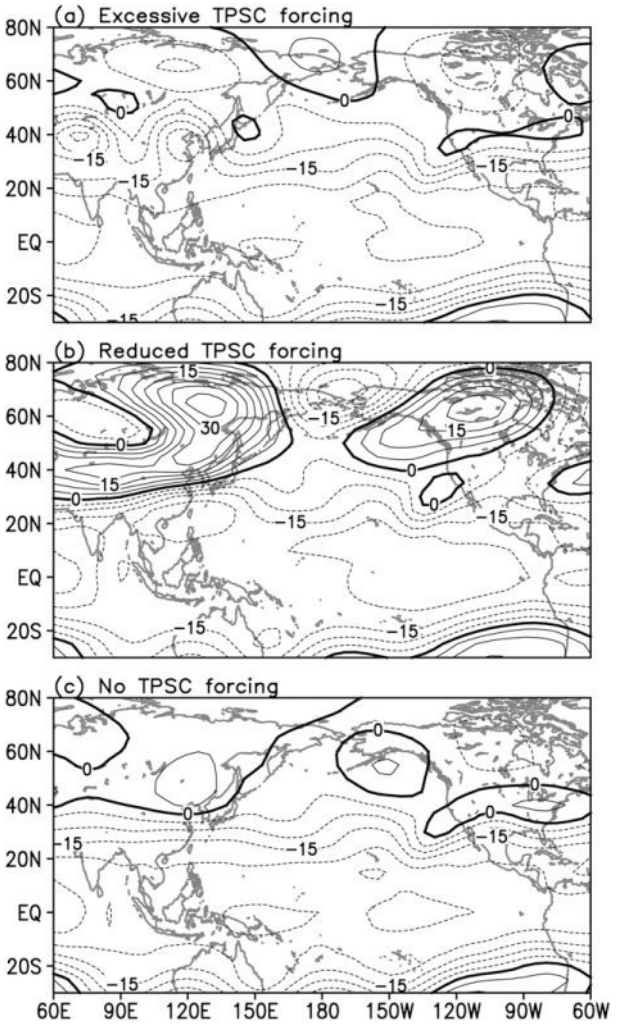

FIG. 10. The SGCM H_{150} responses (contours: gpm) to La Niña with (a) excessive TPSC, (b) reduced TPSC, and (c) no TPSC anomaly forcing in summer.

indicates that the diabatic forcing associated with the anomalous TPSC can modulate the ENSO-related teleconnection patterns and the background zonal mean flows.

To further understand why the background zonal mean flow associated with the reduced TPSC is more favorable for a stronger or westward development of ENSO teleconnections, we calculated the amplitude of the Rossby wave response to ENSO diabatic forcing (e.g., Hoskins and Yang 2000; Lin 2009). For the steady forcing of ENSO, the amplitude of the Rossby wave response meets the following relationship:

$$A = \frac{1}{\sqrt{(\omega_k + kU)^2 + \alpha^2}}, \qquad (1)$$

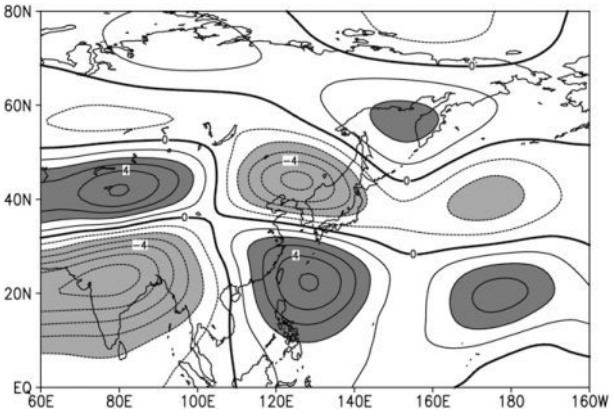

FIG. 11. The 150-hPa zonal wind responses in the SGCM regarding reduced and excessive TPSC forcing in summer (reduced minus excessive).

where ω_k is the wave frequency (which is a function of k according to the dispersion relationship), k the wavenumber, U the basic-state zonal wind, and α the damping. The parameters used in this study include $k = 6$ (equivalent to a typical ENSO forcing scale), $\beta = 2.2 \times 10^{-11}$ m^{-1} s^{-1}, $H = 200$ m, and $\alpha = (10 \text{ day})^{-1}$. According to the aforementioned observational results, U is around 16 m s^{-1} for the reduced TPSC summers and 17 m s^{-1} for the excessive TPSC summers. We computed the amplitude factor A for the high/low TPSI summer, respectively. Results show that, during a low TPSI summer, A is ~8 for Rossby wave mode $n = 1$ and 6.8 for mode $n = 2$. During a high TPSI summer, A is ~7 for Rossby wave mode $n = 1$ and 5.5 for mode $n = 2$. Therefore, A in a low TPSI summer is greater than that in a high TPSI summer. It indicates that the Rossby wave gyre in a reduced TPSC summer has larger amplitudes, which favors a more westward development. This result theoretically proves that the TPSC can modulate ENSO teleconnections through changing the background zonal mean flows.

6. Conclusions

The diabatic forcing associated with the anomalous TPSC is an important driving force of large-scale atmospheric circulation and can exert profound influences to the downstream climate variability (e.g., Wang et al. 2008a; Lin and Wu 2011). This study examined the observed relationship among the TPSC, EASM, and simultaneous ENSO. It is found that the TPSC does show modulating effects on the ENSO teleconnections and, in turn, modifies the ENSO–EASM relationship. Numerical and theoretical evidence confirms that the enhanced relationship between ENSO and the EASM is likely or partly due to the fact that the Rossby wave response to the ENSO diabatic forcing is stronger in a reduced TPSC summer. The contribution from the TPSC provides another physical background to understand the strengthened EASM–ENSO relationship and to predict the long-term variations of the EASM.

It should be pointed out that the TPSC is not the sole contributor to changes in the ENSO teleconnections. Other factors including tropical SST, water vapor, and winds; the NAO; and the NPO can contribute to such a change (e.g., Gershunov and Barnett 1998; Wang et al. 2008d; Yeh et al. 2009; Wu et al. 2012). In addition, the change in the EASM–ENSO relationship may also contribute to the TPSC change (Yim et al. 2008). Its effect can be reflected by modifying the EASM rainfall over the Tibetan Plateau. As a matter of fact, the current TPSC change is a comingled result of natural variations and anthropogenic effects. Given the occurrences of the reduced TPSC could become more frequent with increasing levels of greenhouse gases in the atmosphere in the future (Meehl et al. 2007), we infer that the TPSC may play an increasingly important role in shaping ENSO teleconnections as well as enhancing their connection with the EASM in the next decades.

Acknowledgments. We appreciate the Global Snow Lab (Rutgers University) for providing the snow cover area extent data. Zhiwei Wu is supported by the National Basic Research Program "973" (Grant 2010CB950400), a Project Funded by the Priority Academic Program Development (PAPD) of Jiangsu Higher Education Institutions, and the Special Research Program for Public Welfare (Meteorology) of China (Grant GYHY200906016). We would also like to thank the editor and three anonymous reviewers for improving the original manuscript.

REFERENCES

Chang, C.-P., Y. Zhang, and T. Li, 2000a: Interannual and interdecadal variation of the East Asian summer monsoon rainfall and tropical SSTs. Part I: Roles of the subtropical ridge. *J. Climate,* **13,** 4310–4325.

——, ——, and ——, 2000b: Interannual and interdecadal variation of the East Asian summer monsoon rainfall and tropical SSTs. Part II: Meridional structure of the monsoon. *J. Climate,* **13,** 4326–4340.

Chen, M., P. Xie, J. E. Janowiak, and P. A. Arkin, 2002: Global land precipitation: A 50-yr monthly analysis based on gauge observations. *J. Hydrometeor.,* **3,** 249–266.

Fu, C. B., and X. L. Teng, 1988: Relationship between summer climate in China and El Niño/Southern Oscillation phenomenon (in Chinese). *Chin. J. Atmos. Sci.,* **12,** 133–141.

Gershunov, A., and T. P. Barnett, 1998: Interdecadal modulation of ENSO teleconnections. *Bull. Amer. Meteor. Soc.,* **79,** 2715–2725.

Gill, A. E., 1980: Some simple solutions for heat-induced tropical circulations. *Quart. J. Roy. Meteor. Soc.,* **106,** 447–462.

Hall, N. M. J., 2000: A simple GCM based on dry dynamics and constant forcing. *J. Atmos. Sci.,* **57,** 1557–1572.

Hoskins, B. J., and A. J. Simmons, 1975: A multi-layer spectral model and the semi-implicit method. *Quart. J. Roy. Meteor. Soc.,* **101,** 637–655.

——, and D. J. Karoly, 1981: The steady linear response of a spherical atmosphere to thermal and orographic forcing. *J. Atmos. Sci.,* **38,** 1179–1196.

——, and G. Y. Yang, 2000: The equatorial response to higher-latitude forcing. *J. Atmos. Sci.,* **57,** 1197–1213.

——, M. E. McIntyre, and A. W. Robertson, 1985: On the use and significance of isentropic potential vorticity maps. *Quart. J. Roy. Meteor. Soc.,* **111,** 877–946.

Kalnay, E., and Coauthors, 1996: The NCEP/NCAR 40-Year Reanalysis Project. *Bull. Amer. Meteor. Soc.,* **77,** 437–471.

Kwon, M. H., J.-G. Jhun, and K.-J. Ha, 2007: Decadal change in East Asian summer monsoon circulation in the mid-1990s. *Geophys. Res. Lett.,* **34,** L21706, doi:10.1029/2007GL031977.

Li, J., Z. Wu, Z. Jiang, and J. He, 2010: Can global warming strengthen the East Asian summer monsoon? *J. Climate,* **23,** 6696–6705.

Lin, H., 2009: Global extratropical response to diabatic heating variability of the Asian summer monsoon. *J. Atmos. Sci.,* **66,** 2697–2713.

——, and J. Derome, 1996: Changes in predictability associated with the PNA pattern. *Tellus,* **48A,** 553–571.

——, and Z. Wu, 2011: Contribution of the autumn Tibetan Plateau snow cover to seasonal prediction of North American winter temperature. *J. Climate,* **24,** 2801–2813.

Meehl, G. A., and Coauthors, 2007: Global climate projections. *Climate Change 2007: The Physical Science Basis,* S. Solomon et al., Eds., Cambridge University Press, 747–845.

Pu, Z. X., L. Xu, and V. V. Salomonson, 2007: MODIS/*Terra* observed seasonal variations of snow cover over the Tibetan Plateau. *Geophys. Res. Lett.,* **34,** L06706, doi:10.1029/2007GL029262.

Shaman, J., and E. Tziperman, 2005: The effect of ENSO on Tibetan Plateau snow depth: A stationary wave teleconnection mechanism and implications for the South Asian monsoons. *J. Climate,* **18,** 2067–2079.

Smith, T. M., and R. W. Reynolds, 2004: Improved extended reconstruction of SST (1854–1997). *J. Climate,* **17,** 2466–2477.

Tao, S., and Y. Ding, 1981: Observational evidence of the influence of the Qinghai-Xizang (Tibet) Plateau on the occurrence of heavy rain and severe convective storms in China. *Bull. Amer. Meteor. Soc.,* **62,** 23–30.

Wang, B., R. Wu, and X. Fu, 2000: Pacific–East Asia teleconnection: How does ENSO affect East Asian climate? *J. Climate,* **13,** 1517–1536.

——, Q. Bao, B. Hoskins, G. Wu, and Y. Liu, 2008a: Tibetan Plateau warming and precipitation change in East Asia. *Geophys. Res. Lett.,* **35,** L14702, doi:10.1029/2008GL034330.

——, and Coauthors, 2008b: How accurately do coupled climate models predict the Asian–Australian monsoon interannual variability? *Climate Dyn.,* **30,** 605–619.

——, Z. Wu, J. Li, J. Liu, C.-P. Chang, Y. Ding, and G.-X. Wu, 2008c: How to measure the strength of the East Asian summer monsoon? *J. Climate,* **21,** 4449–4463.

——, J. Yang, T. Zhou, and B. Wang, 2008d: Interdecadal changes in the major modes of Asian–Australian monsoon variability: Strengthening relationship with ENSO since the late 1970s. *J. Climate,* **21,** 1771–1789.

——, F. Huang, Z. Wu, J. Yang, X. Fu, and K. Kikuchi, 2009: Multi-scale climate variability of the South China Sea monsoon: A review. *Dyn. Atmos. Oceans,* **47,** 15–37.

Weng, H. Y., K. M. Lau, and Y. Xue, 1999: Multi-scale summer rainfall variability over China and its long-term link to global sea surface temperature variability. *J. Meteor. Soc. Japan,* **77,** 845–857.

Wu, R., and B. P. Kirtman, 2007: Observed relationship of spring and summer East Asian rainfall with winter and spring Eurasian snow. *J. Climate,* **20,** 1285–1304.

Wu, Z., and J. Li, 2008: Prediction of the Asian-Australian monsoon interannual variations with the grid-point atmospheric model of IAP LASG (GAMIL). *Adv. Atmos. Sci.,* **25,** 387–394.

——, B. Wang, J. Li, and F.-F. Jin, 2009: An emperical seasonal prediction model of the East Asian summer monsoon using ENSO and NAO. *J. Geophys. Res.,* **114,** D18120, doi:10.1029/2009JD011733.

——, J. Li, Z. Jiang, J. He, and X. Zhu, 2012: Possible effects of the North Atlantic Oscillation on the strengthening relationship between the East Asian summer monsoon and ENSO. *Int. J. Climatol.,* doi:10.1002/joc.2309, in press.

Yang, S., and K. M. Lau, 2006: Interannual variability of the Asian monsoon. *The Asian Monsoon,* B. Wang, Ed., Springer/Praxis Publishing Ltd., 259–293.

Ye, D., 1981: Some characteristics of the summer circulation over the Qinghai-Xizang (Tibet) Plateau and its neighborhood. *Bull. Amer. Meteor. Soc.,* **62,** 14–19.

Yeh, S. W., J. S. Kug, B. Dewitte, M. H. Kwon, B. P. Kirtman, and F. F. Jin, 2009: El Niño in a changing climate. *Nature,* **461,** 511–514.

Yim, S., S. Yeh, R. Wu, and J. Jhun, 2008: The influence of ENSO on decadal variations in the relationship between the East Asian and western North Pacific summer monsoons. *J. Climate,* **21,** 3165–3179.

Yonetani, T., 1992: Discontinuous changes of precipitation in Japan after 1900 detected by the Lepage test. *J. Meteor. Soc. Japan,* **70,** 95–104.

Zhang, Y., T. Li, and B. Wang, 2004: Decadal change of the spring snow depth over the Tibetan Plateau: The associated circulation and influence on the East Asian summer monsoon. *J. Climate,* **17,** 2780–2793.

Zhu, X., J. He, and Z. Wu, 2007: Meridional seesaw-like distribution of the Meiyu rainfall over the Changjiang–Huaihe River Valley and characteristics in the anomalous climate years. *Chin. Sci. Bull.,* **52,** 2420–2428.